Characteristics of Stationary Closed Streamlines in Stratified Fluids Part 2 : Experiments of the Vortex Pair

By Masafumi KAMACHI*, Kesayoshi HADANO*
and Hiroyuki HONJI**

(Received July 12, 1985)

Absract

The Prandtl–Batchelor theorem for a stratified fluid is applied to the internal solitary vortex pair. The experimental data of the internal vortex pair show that the density and the vorticity are homogeneous in the vortex pair.

1. Introduction

Gravity currents have been studied extensively in hydraulics (e.g. Tamai[1]).Many observations of internal solitary waves also have been reported[2)–11)], and they have many problems in studies of the geophysical fluid dynamics[12),13)] and of the ocean structures : when we construct deep–water oil drilling and production facilities, we will have to build the structures that can withstand the large horizontal wave forces generated by the internal solitary waves[9),10),14)].Gravity currents and internal solitary waves seem to have been investigated separately. As reported in a preceding paper[15)], it has been observed that a gravity current evolves into an internal solitary wave. The studies about the two phenomena, therefore, will be combined. Internal solitary bulges, which have been investigated extensively (e.g. Maxworthy[13)]), seem to have a close connection with the gravity currents, especially, a closed region of a current head ; by bulges we mean internal solitary waves and internal solitary vortex pairs inclusively.

Flow visualization techniques have been used in several studies of the internal solitary bulge. Almost all the studies, however, demonstrated only unsteady flow patterns viewed by an observer at rest with respect to tank filled with water in which a bulge propagates. The inherent structure of the bulge may will be revealed by resorting directly to steady flow patterns viewed by an observer moving with the bulge. Generally, unsteady flow patterns need great care in their interpretation. Some possible pitfalls arising in their interpretation have been pointed out[16)–18)†].Steady streamline patterns, therefore, have been demonstrated of a solitary bulge forming on an interfacial transition region in fresh and salt water[19)].The bulge is composed of a vortex pair when the amplitude of the bulge is large.

*Department of Civil Engineering
**Research Institute for Applied Mechanics, Kyushu University.

†In Bradshaw's text, the first figure of Fig. 41 in p. 147 contains an error. The wave length in the figure which shows travelling–wave streamlines seen by stationary observer should be divided by a factor 2.

As reported in the Part 1 of papers about the Prandtl–Bactchelor theorem for stratified fluids[20], some papers have devoted to extensions of the theorem. Although the theorem have been confirmed, they have been confined to analytical and numerical analyses. Therefore, "laboratory" experimental data seem to be necessary in order to reveal and confirm the theorem. The aim of this paper is an application of the theorem to a result of laboratory experiments of the internal solitary bulge.

Experimental method are described in Section 2. Finally, we discuss the results of the internal solitary bulge and application of the Prandtl–Batchelor theorem in Section 3.

2. Eeperimental Apparatus and Method

The experiments were carried out using a water tank illustrated schematically in Fig. 1. The tank was made of acrylic resin, *2.0 m* long, *25 cm* deep, and *20 cm* wide. The

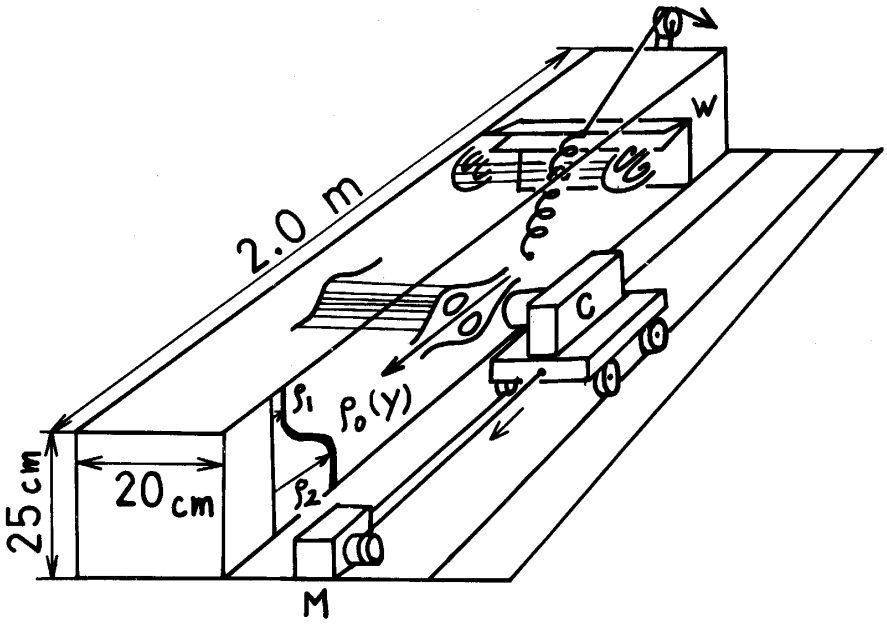

Fig. 1 Experimental apparatus. *C*: 35 mm camera, *M*: motor, *W*: wavemaker.

water was stratified by letting a brine flow into the bottom of a fresh-water with mean density ρ_1, which initially half filled the tank. The distribution of the density is obtained with a handmade probe of the electric conductivity (cf. Gibson and Schwartz[21]; Mide and Merceret[22]). The profile is approximately of the hyperbolic–tangent type: $\rho = \bar{\rho}\ (1-\delta\ \tanh \alpha Y)$, where $\bar{\rho} = (\rho_1+\rho_2)/2$, $\delta = (\rho_2-\rho_1)/(\rho_2+\rho_1)$, ρ_2 is the mean density of the lower brine ranging from *1.01* to *1.10* gcm^{-3}, and α is the inverse of a half of the density transition layer thickness ranging from *0.35* to *1.0 cm*. A typical profile of salinity distribution is shown in Fig. 2. In the figure the profiles are those measured before and after the experiment. The profiles are almost the same as with each other. Therefore, the mixing of the density which is due to the propagation of the vortex pair is small compared with $\bar{\rho}$.

The tank was equipped with a wavemaker of two hinged plates of a bivalved hinge

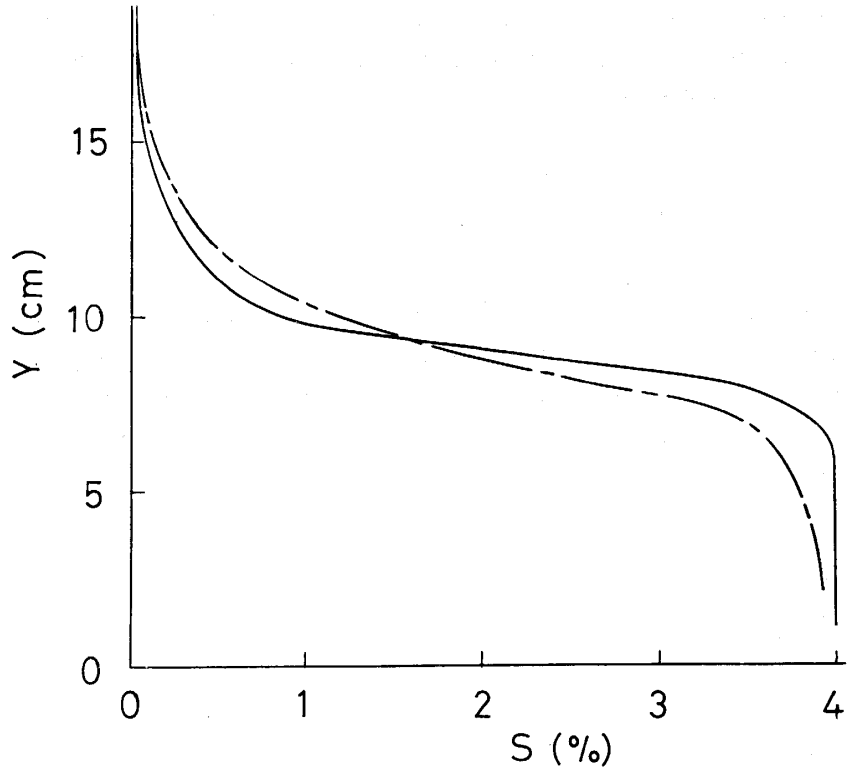

Fig. 2 Salinity S % vs depth Y *cm*. Solid and broken line show salinity distributions before and after an experiment, respectivelv.

were placed at one end of the tank. It spanned the inside width of the tank at the transition layer level. The plates were opened at some angle initially and were banged with a rubber spring. A lump of salt water was kicked out along the transition layer to produce the embryo of a bulge. This embryo was initially like the head of a gravity current. At about 20 cm downstream of the hinge, however, an internal solitary wave or vortex pair formed. Formulation of an internal solitary wave or vortex pair depended on the angle between two hinged plates.

Photographes of steady streamline patterns of a propagating bulge were taken with a 35 mm camera. The camera was controlled to move at the nearly same speed as the propagating speed of the bulge by use of a rail and carriage system of a motor, which is installed outside the tank. Flow visualization was carried out by use of aluminum flakes and wet sawdusts slightly heavier than the fresh water.

The viscosity of fluids have an effect on a gradual decay of the bulges. Such a decay can not be perceived during the first one–way of the bulges from one end to the other of the tank.

3. Results and Discussions

Photographs of flow patterns of bulges are the same as those shown in a paper by

Kamachi and Honji[19]. It is difficult that we calculate the vorticity from the photograph directly, because the vorticity contains space derivatives of the velocity. Using a photograph of the steady streamlines of the vortex pair we evaluate the vorticity as follows. The vorticity is related with cirulation :

$$\omega_i = \frac{1}{A_i} \oint_{\xi} u \cdot \mathrm{d}\xi \ , \tag{3.1}$$

where A_i is an area of a closed region, and hereafter suffix i denotes the number of the closed streamline region. We approximate the shape of the closed region as an ellipse and the velocity as a locus of an alumlnum flake, l_j, divided by an exposure time T (in our experiments $T = 1$ s). A shape and notations are shown schematically in Fig. 3.

We evaluate the circulation as

$$\Gamma_i = \oint_{\xi} u \cdot \mathrm{d}\xi \fallingdotseq \sum_j \frac{l_j^2}{T} \ , \tag{3.2}$$

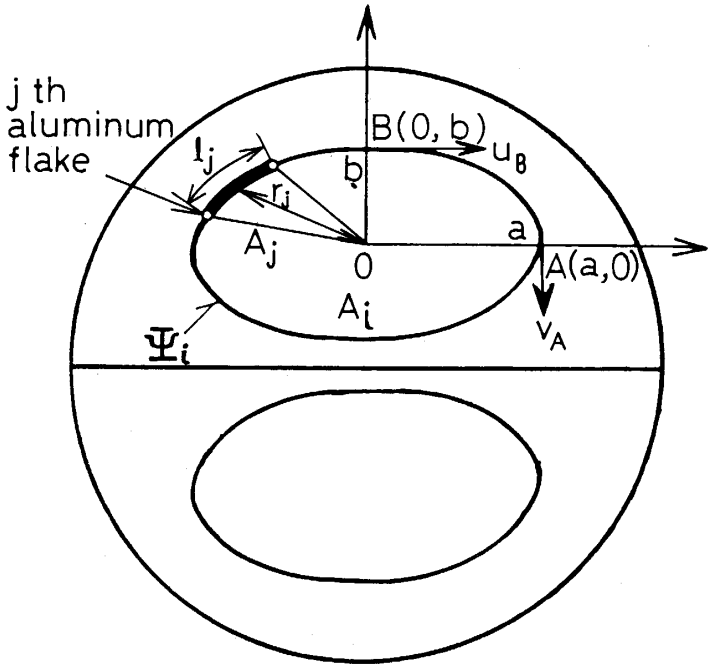

Fig. 3 Schematic diagram of a vortex pair.

where suffix j represents the number of the locus of the alumlnum flakes on ith streamline, and the summation is taken about the total length of the streamline (i.e. the summation of l_j must be the circuit length of the ellipse). In photographs taken in our experiments, there are one or two loci on one streamline. We must, therefore, infer the values of the circulation along a part of the streamline on which the locus of the aluminum flake does not appear. Then we assume the conservation of the angular momentum on one streamline.We should notice that this assumption does not mean that the Prandtl–Batchelor theorem is correct *a priori*, because the theorem represents a relation of the vorticity on the "different" streamlines. The above assumption may be correct with two reasons : (1) As discussed about Eq. (2. 4) in the Part 1, ω is the function of stream function only. Therefore, the vorticity is constant along one streamline. It is the conservation of the angular momentum on one streamline. (2) By use of the experimental data which are shown in Table 1 with analyzed data, we evaluate areas of two fan–shaped regions which consist of a center of the closed region and loci of the aluminum flakes. In Table 1

Table 1 Experimental and the analyzed data. Suffix i is omitted for simplicity. Data of No. 1 to 11 are obtained in upper side regions of the vortex pair, and other data are for the lower regions.

DATA NO.	r (cm)	l (cm)	a (cm)	b (cm)	A (cm^2)	L (cm)	$\lvert\omega\rvert$ (s^{-1})
1	1.61	0.375	1.61	0.513	2.60	7.13	17.6
2	1.44	0.375	1.50	0.475	2.24	6.63	17.5
3	1.38	0.400	1.38	0.438	1.90	6.10	17.2
4	1.00	0.288	1.01	0.363	1.15	4.56	15.9
5	0.813	0.313	0.953	0.313	0.937	4.24	16.5
6	0.750	0.275	0.750	0.263	0.620	3.37	16.6
7	2.13	0.463	2.20	0.688	4.76	9.71	18.0
8	0.288	0.125	0.360	0.125	0.141	1.61	15.9
9	2.03	0.425	2.03	0.619	3.95	8.92	18.3
10	0.375	0.750	1.33	0.475	1.98	6.00	14.2
11	0.625	0.800	1.35	0.438	1.86	5.99	14.8
12	1.975	0.375	2.33	0.800	5.86	10.4	17.3
13	2.06	0.450	2.42	0.825	6.27	10.8	17.2
14	2.25	0.400	2.50	0.875	6.87	11.2	17.1
15	2.50	0.400	2.50	0.875	6.87	11.2	17.1
16	1.13	0.725	2.94	0.938	8.66	13.0	17.5
17	0.875	0.725	2.07	0.650	4.23	9.14	16.9
18	1.20	0.775	2.50	0.875	6.87	11.2	16.0
19	0.750	0.663	1.62	0.556	2.83	7.25	15.5
20	0.525	0.563	1.22	0.425	1.63	5.49	15.1
21	1.00	0.625	1.38	0.600	2.60	6.46	13.3
22	1.01	0.663	2.33	0.800	5.86	10.4	16.4

the data (No. *14* and *18*) are measured on the same streadmline. Using the values of r and l, we have the area of No. 14 is *0.800* cm^2 and *0.781* cm^2 for No. 18. Therefore, the areas are almost the same. This result means that the Kepler's third law is realized in the fluid and the angular momentum is conserved. Using the above angular momentum conservation we evaluate the circulation. In all areas which do not contain the fan-shaped region in one ellipse enclosed by one stremline, we estimate a length of the circle as $(A-A_j) / r_i$ which shape is transformed from the areas to a supposed fan-shaped area by use of the angular momentum conervation ($A_j \fallingdotseq r_j l_j$ is the area of the fan-shaped region enclosed by a locus of an aluminum flake and radii, and r_j is a supposed radius between the center of the ellipse and the circle in the supposed fan-shaped region). We have therefore

$$\Gamma_i \fallingdotseq \frac{1}{T}\left[l_j^2+\left(\frac{A-A_j}{r_i}\right)^2\right] \tag{3.3}$$

$$= \frac{1}{T}\left[l_j^2+(L_i-l_j)^2\right], \tag{3.4}$$

in which we used $r_i = (A-A_j) / (L_i-l_j)$, L_i is a length of the circle around ith ellipse,

$$L_i = 4a_i E(e_i^2), \tag{3.5}$$

$$e_i^2 = (a_i^2-b_i^2) / a_i^2, \tag{3.6}$$

$$E(e_i^2) = \int_0^{\pi/2} (1-e_i^2 \sin^2\theta)^{1/2} d\theta \tag{3.7}$$

is the complete elliptic integral of the second kind [23], and (a_i, b_i) are the lengths of the long and short axes of the ellipse, respectively. According to the above discussion we have

$$|\omega_i| \fallingdotseq \frac{|\Gamma_i|}{A_i}, \tag{3.8}$$

where $A_i = \pi a_i b_i$ · If ω_i has a constant value for all i, the Prandtl-Batchelor theorem is realized.

The values of the vorticity against the area are shown in Fig. 4. This figure shows that the vorticity of a closed region in an upper or a lower side of the vortex pair is almost constant. The values of the data are slightly scattered, because the above analysis has some errors : (1) The shape of the upper and the lower side of the vortex pair is not exactly ellipse. (2) The photographs were taken in a slit, which width is about 7 mm, of the light source. The aluminum flakes may go out from the width of the slit in the exposure time, since the motion may not be two dimensional or the motion may have weak disturbances. (3) The values of the vorticity depend on the value in the boundary layer (g.u.

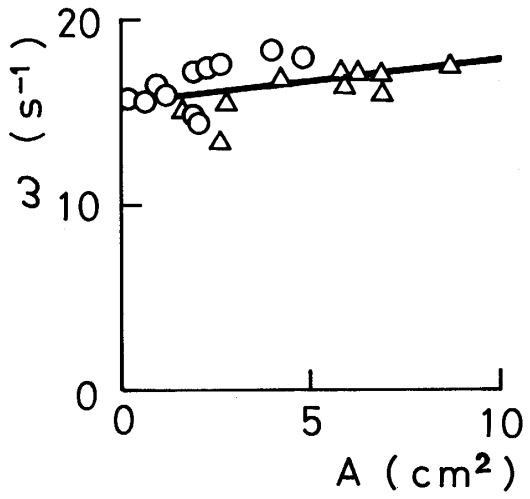

Fig. 4 Vorticity ω plotted against area A. (○) Data in upper side regions of the vortex pair, (△) in lower side regions. The straight line is $\omega = 15.5 + 0.229A$ which is obtained with the least square method. Small value of the coefficient of A implies that the Prandtl–Batchelor theorem is realized.

Grimshaw[24] for the thermal boundary layer). The vortex pair with the boundary layers of the upper and the lower side regions is not made symmetrically by the wavemaker.

If we solve a relation between the constant vorticity, ω_0, and the steady stream function Ψ_i :

$$\frac{\partial^2 \Psi_i}{\partial X^2} + \frac{\partial^2 \Psi_i}{\partial Y^2} = -\omega_0 , \tag{3.9}$$

in the ellipse, we get a solution

$$\Psi_i = -\frac{1}{2}\omega_0 \left(\frac{X^2}{a_i^2} + \frac{Y^2}{b_i^2}\right) \Big/ \left(\frac{1}{a_i^2} + \frac{1}{b_i^2}\right) . \tag{3.10}$$

The solution is general and obtained originally in a homogeneous fluid (e.g. Wood [25]). If we plot the flow pattern using the above solution, we may note that the flow pattern is similar to that of the photograph and Fig. 1 in the Part 3. Using above solution we get velocities at A $(a, 0)$, B $(0, b)$ on the long and the short axes, u_A, u_B :

$$u_A = \omega_0 / \left[\left(\frac{1}{a^2}+\frac{1}{b^2}\right) a\right] , \tag{3.11}$$

$$u_B = \omega_0 / \left[\left(\frac{1}{a^2}+\frac{1}{b^2}\right) b\right] . \tag{3.12}$$

We have, therefore, a ratio of the two velcocities as

$$\frac{|u_A|}{|u_B|} = \frac{b}{a} . \tag{3.13}$$

In the experimental data (No. 12 and 22 in Table 1), we have $|u_A| = 0.375\ cm\ s^{-1}$, $|u_B| = 0.663\ cm\ s^{-1}$. From these data, we get $|u_A/u_B| = 0.566$, $b/a = 0.473$. From the data, therefore, Eq. (3.13) is in reality. The error may be due to the measurements of a and b on the photograph.

Figure 5 shows that a typical output signal of electric conductivity in and around

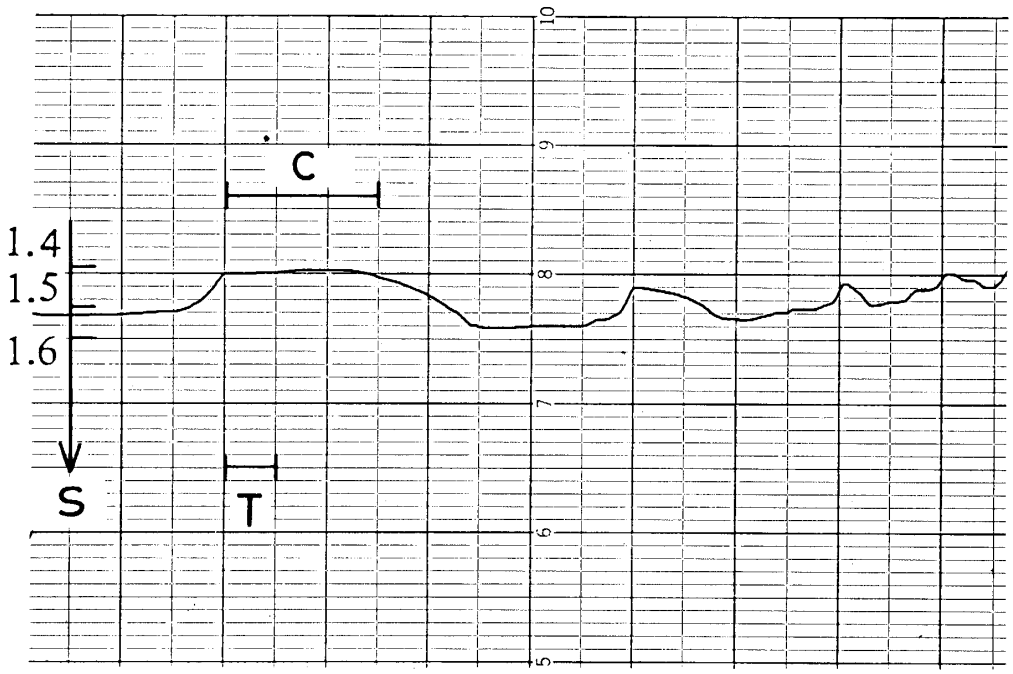

Fig. 5 Output signal of the electric conductivity in and around the vortex pair plotted against time.
C : closed region, S : salinity (%), T : time (s). Time scale = 1.7 s.

the vortex pair. The figure seems to reveal the homogeneous density in the vortex pair. Behind the vortex pair internal waves are induced.

Figure 6 shows, with some different vortex pairs, a relation between amplitude parameter αA_m and a wave speed parameter λ, where $\lambda = g\ ln\ (\rho_2/\rho_1)/2\ \alpha\ c^2{}_i$, c_i the speed of the vortex pair and g the acceleration due to gravity. The nondimensionalized speed of the vortex pair may be independent of the amplitude parameter. The vortex

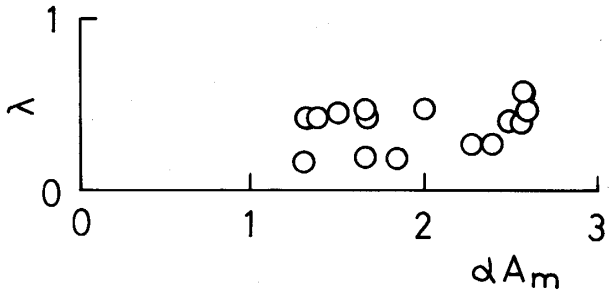

Fig. 6 Wave speed parameter λ plotted against amplitude parameter αA_m.

speed c_i is estimated $\Gamma_i/2\pi D_i$, where D_i is a distance between centers of the upper and the lower closed regions, and $c_i \propto \Gamma_i/\sqrt{A_i}$: From the figure C_i is almost constant so that $\Gamma_i \propto \sqrt{A_i}$: We get, there fore, $\omega_i \propto \Gamma_i/A_i \propto A_i^{-1/2}$: The arqument above mentioned means that the values of the vorticity in different vortex pairs with different amplitudes are not equal one another. The reason of the different values of the vorticties is that the values gained by the Prandtl–Batchelor therorem depend on the vortex boundary layer as mentioned about Fig. 4.

For the stratified fluid flow the Prandtl–Batchelor theorem may be confirmed with these figures 4 and 5.

Acknowledgements

We are indebted to Prof. T. Saitou for useful discussion. We also would like to express our thanks to Dr. A. Masuda (Kyushu University) for the data analysis and to Dr. J. S. Turner (Australian National University) for a useful suggestion about Fig. 6.

References

1) Tamai, N. "Mitsudoryu no Suiri" (Gihoudou) p. 260 (1980) (in Japanese)
2) Gaul, R. D. "Observations of Internal Waves near Hudson Canyon", J. Geophys. Res., **66**, 3821–3830 (1961)
3) Perry, R. B. and Schimke, G. R. "Large–Amplitude Internal Waves Observed off the Northwest Coast of Sumatra", J. Geophys. Res., **70**, 2319–2324 (1965)
4) Ziegenbein, J. "Spatial Observations of Short Internal Waves in the Strait of Gibraltar", Deep–Sea Res., **17**, 867–875 (1970)
5) Halpern, D. "Observations on Short–Period Internal Waves in Massachusetts Bay", J. Mar. Res., **29**, 116–132 (1971)
6) Hunkins, K. and Fliegel, M. "Internal Undular Surges in Seneca Lake : A Natural Occurrence of Solitons", J. Geophys. Res., **78**, 539–548 (1973)
7) Lee, C.–Y. and Beardsley, R. C. "The Generation of Long Nonlinear Internal Waves in a Weakly Stratified Shear Flow", J. Geophys. Res., **79**, 453–462 (1974)

8) Christie, D. R., Muirhead, K. J. and Hales, A. L. "On Solitary Waves in the Atmosphere", J. Atmos. Sci., **35**, 805–825 (1978)
9) Osborne, A. R., Burch, T. L. and Scarlet, R. I. "The Influence of Internal Waves on Deep–Water Drilling", J. Pet. Technol., **30**, 1497–1404 (1978)
10) Osborne, A. R. and Burch, T. L. "Internal Solitons in the Andaman Sea", Science, **208**, 451–460 (1980)
11) Apel, J. R. and Holbrook, J. R. "The Sulu Sea Internal Soliton Experiment, Part a ; Background and Overview", EOS., **61**, 1009 (1980)
12) Maxworthy, T. "Non–Linear, Dispersive Waves in the Laboratory and in Nature", In : B. J. West (editor) Nonlinear Properties of Internal Waves, AIP Conference Proceedings, **76**, 11–46 (1981)
13) Maxworthy, T. "Solitary Waves on Density Interfaces", In : R. E. Meyer (editor) Waves on Fluid Interfaces, 201–220 (1983)
14) BMS. "Great Undersea Waves May be Solitons", Phys. Today, Nov., 20–22 (1980)
15) Honji, H. and Kamachi, M. "The Generation of Internal Solitary Disturbances by Gravity Gurrents in a Stratified Fluid", Rep. Res. Inst. Appl. Mech., Kyushu Univ., **29**, 13–25 (1981)
16) Hama, F. R. "Streaklines in a Perturbed Shear Flow", Phys. Fluids, **5**, 644–650 (1962)
17) Tritton, D. J. "Physical Fluid Dynamics" (Van Nostland Reinhold Comp.) p. 362 (1977)
18) Bradshaw, P. "Experimental Fluid Mechanics" (Pergamon Press)p. 219 (1964)
19) Kamachi, M. and Honji, H. "Steady Flow Patterns of Internal Solitary Bulges in a Stratified Fluid", Phys. Fluids, **25**, 1119–1120 (1982)
20) Kamachi, M., Saitou, T. and Honji, H. "Characteristics of Stationary Closed Streamline in Stratified Fluids, Part 1 : Theory of Laminar Flows", Tech. Rep. Yamaguchi Univ., **3**, 295–304(1985)
21) Gibson, C. H. and Schwartz, W. H. "Detection of Conductivity Fluctuations in a Turbulent Flow Field", J. Fluid Mech., **16**, 357–364 (1963)
22) Mied, R. P. and Merceret, Jr., F. J. "The Construction of a Simple Conductivity Probe", Tech. Note, Dept. Mech. Johns Hopkins Univ., 1–27 (1968)
23) Abramowitz, M. and Stegun, I. A. (Editor)"Handbook of Mathematical Functions", (Dover Pub.) p. 1046 (1984)
24) Grimshaw, R. H. J. "On Steady Recirculating Flows", J. Fluid Mech., **39**, 695–703 (1969)
25) Wood, W. W. "Boundary Layers Whose Streamlines are Closed", J. Fluid Mech., 2, 77–87 (1957)